Automatic detection and branch switching methods for steady bifurcation in fluid mechanics

Yann Guevel, Hassan Boutyour, Jean-Marc Cadou

Automatic detection and branch switching methods for steady bifurcation in fluid mechanics

Y. Guevel [a], H. Boutyour [b], J.M. Cadou [a]

[a] *Laboratoire d'Ingénierie des Matériaux de Bretagne, Université Européenne de Bretagne, Université de Bretagne Sud, Rue de Saint Maudé, B.P. 92116, 56321 Lorient Cedex, France*

[b] *Département de Physique Appliquée, Faculté des Sciences et Technique, Université Hassan I, B.P. 577, Settat, Morocco*

This paper deals with the computation of steady bifurcations in the framework of 2D incompressible Navier–Stokes flow. We first propose a numerical method to accurately detect the critical Reynolds number where this kind of bifurcation appears. From this singular value, we introduce a numerical tool to compute all the steady bifurcated branches. All these algorithms are based on the Asymptotic Numerical Method [1,2]. The critical values are determined by using a bifurcation indicator [3–5] and the bifurcated branches are computed by using an augmented system which was first introduced in solid mechanics [4,6]. Several numerical examples from 2D Navier–Stokes show the reliability and the efficiency of the proposed methods.

1. Introduction

The study of flow stability is an exciting challenge as fluid flow exhibits a lot of bifurcation phenomena, such as steady or Hopf bifurcations. The former generally leads to a loss of symmetry in the flow, whereas the latter designates the transition between a steady to a time-periodic flow. In the present paper, we study the first kind of instability within the framework of 2D incompressible Navier–Stokes equations. More precisely, only numerical methods to detect and study such instabilities are considered in this work. The objective of this paper is to define accurate and efficient methods to firstly compute bifurcation points and secondly follow the bifurcated nonlinear solutions. In fluid mechanics, to our knowledge, few numerical methods exist to treat this kind of problem. Nevertheless, a lot of results (numerical or experimental) on these topics can be found in the literature. For example, the stability of the flow in a channel with sudden expansion has been largely investigated (see, for example, [7–9]). For this example, the influence of the geometric parameters (the expansion ratio) on the critical Reynolds numbers is studied. These critical Reynolds numbers are numerically determined either by computing the eigenvalues of the tangent operator [7] or by perturbing a stationary solution and then verifying if this solution returns to the original solution or not (see [8,10,11]). In this case, the perturbed problem is generally time-dependent and requires some specific numerical algorithms to limit the computational times (see, for example, [11]). To determine bifurcation points, one can also compute the eigenvalues of the linearized perturbed problems by using some specific and well-adapted eigensolvers, such as the Arnoldi method (see, for example, [7]). In this reference, the authors also check the sign of the determinant of the tangent operator to see if a turning or a bifurcation appears in the flow.

Once the bifurcation points are determined, the computation of bifurcated nonlinear branches is generally realized with the help of a predictor–corrector method [7], the most useful being the Newton–Raphson iterative scheme. An alternative of these incremental-iterative methods is the Asymptotic-Numerical Method (ANM). ANM consists of the association of a perturbation technique and a spatial discretization method, generally the finite element method, and has been successfully applied in nonlinear solid mechanics [1] or in fluid mechanics [2,12]. The advantage of such a method is that it makes it possible to determine analytical nonlinear solutions with computational CPU times lower than with the classical incremental-iterative method. On these nonlinear solutions, some bifurcation indicators have been introduced. Two types of bifurcation can then be considered: stationary and Hopf bifurcation [3,13]. The detection of the two kinds of bifurcations is realized by using the same numerical techniques. Nevertheless, as for the Hopf bifurcation, the computational time to detect accurate values of critical Reynolds numbers is relatively significant, the bifurcation indicator is in this case coupled with a Newton method to considerably decrease the computational cost (see [13]).

As for the steady solution, the indicator was first introduced for solid mechanics [4,6,15,16] and then for the Navier–Stokes equations [3,5,17]. The bifurcation indicator, which is a scalar, results from a perturbation load applied to the steady equations. Finding the bifurcation points then consists in determining where this indicator becomes null along the nonlinear solution branches. In Refs. [4,6], in the case of nonlinear thin shell problems, the bifurcation indicator is computed along the stationary solution using a perturbation method. The indicator is then explicitly known and this enables the easy computation of its roots and finally the bifurcation points. In fluid mechanics studies, this indicator is computed at each Reynolds number and the detection of bifurcation points is realized by using a bisection method to find the critical Reynolds number where the indicator becomes null [3,5]. In this work, as in solid mechanics applications, this indicator is computed via a perturbation method. The computation of bifurcation points is then automatically done by considering the zero of this scalar function. When these bifurcation points are determined, the bifurcated branches are computed by using a numerical method which is also based on the ANM. The branch switching method was firstly introduced within a solid mechanics framework (see [4,6]) and is adapted in this study to the specificity of fluid mechanics problems.

Finally, in this paper we propose some numerical tools which help compute the fundamental solutions, the steady bifurcation point and the resulting nonlinear bifurcated branches. All these numerical developments are based on the ANM and lead to the solutions without large computing CPU times. This is mostly due to the fact that, for all the computations, polynomial approximations are replaced by equivalent rational fractions, the Padé approximants [18,19], which help considerably increase the range of validity of asymptotic expansions.

The present paper is organized as follows. In Section 2, the steady Navier–Stokes equations are written in a well-adapted form for the introduction of the asymptotic expansions. Section 3 is devoted to the stability analysis and notably to the introduction of our steady bifurcation indicator. In the following section, the basis of the ANM are recalled and introduced in the steady and perturbed problem. In Section 5, we give some details about the numerical algorithm used in this study to compute accurate bifurcation points. Section 6 deals with the computation of the bifurcated nonlinear solutions. Next, in Section 7, the spatial discretization used in this work is presented. The discrete operators required for the computation of the fundamental solution, the bifurcation points and the bifurcated branches are also defined in this section. In the following part (Section 8), all the previous developments are applied to classical numerical examples in fluid mechanics which exhibit steady bifurcations. These examples (flow in a sudden expansion or flow in a channel) permit us to show the efficiency and the reliability of all the numerical methods introduced in this study.

2. Governing equations

The steady Navier–Stokes equations for a Newtonian and incompressible fluid are the following:

$$\begin{cases} -\nu u_{i,jj} + u_j u_{i,j} + \frac{1}{\rho} p_{,i} = 0 \quad \text{in } \Omega \\ u_{i,i} = 0 \quad \text{in } \Omega \\ u = \lambda u_d \quad \text{on } \partial_u \Omega \end{cases} \tag{1}$$

where u and p are respectively the velocity and the pressure, u_d is the imposed velocity on the boundary $\partial_u\Omega$ and λ is a control parameter which can be identified as the Reynolds number of the flow. The previous problem is written under the following operator form:

$$L(U) + Q(U,U) = \lambda F \quad \text{in } \Omega \tag{2}$$

where U is a mixed unknown vector (composed of the velocity and the pressure field). The right-hand side, λF, represents the imposed velocity which is modified in the discretized step into a load vector. For the sake of simplicity, this transformation is introduced into the previous equation which is written in a continuous frame. The linear operator $L(U)$ represents the Laplacian and the divergence operator of Eq. (1). The quadratic operator $Q(U,U)$ designates the convective term of the steady Navier–Stokes equations. Usually, the nonlinear problem (2) is solved by using an incremental iterative method, the most popular being the Newton–Raphson iteration scheme. Nevertheless, in this study, the Asymptotic Numerical Method, which has proved its efficiency in solid mechanics problems [1] or in fluid mechanics [2], is preferred.

3. Linear stability analysis

Once the nonlinear solution is computed, its stability can be discussed. In this paper on steady bifurcation, which generally indicates a loss of symmetry in the flow, the stability analysis is studied by introducing a bifurcation indicator. This indicator has already been introduced in fluid mechanics [3,5] and has been initially developed for solid mechanics problem [4,6].

To make this paper self-contained, we firstly recall how this indicator is introduced. The steady Navier–Stokes solution, denoted by U^λ, is perturbed by a load vector μf where μ is the intensity and f is a random vector. The consequence for the flow is a fluctuation in the velocity, ΔU which is written:

$$U = U^\lambda + \Delta U \tag{3}$$

By considering the previous relation and the perturbation vector μf, the indicator μ and the stationary solution can be computed by the following nonlinear system of equations:

$$\begin{cases} L(U^\lambda) + Q(U^\lambda, U^\lambda) = \lambda F \\ L(\Delta U) + Q(\Delta U, U^\lambda) + Q(U^\lambda, \Delta U) = \mu f \\ \langle \Delta u - \Delta u_0, \Delta u_0 \rangle = 0 \end{cases} \tag{4}$$

The first equation of the previous system represents the classical stationary Navier–Stokes equations (i.e. Eq. (2)) and the second one is the linear stability equation. In the latter, the second order term in ΔU is neglected. As the number of unknowns is greater than the number of equations, a normalization condition is added to get a well posed problem. The supplementary equation is the last one of the system (4). In this third equation, the initial perturbed vector, ΔU_0, is a solution of the perturbed problem where μ is designated as equal to 1:

$$L_t(\Delta U_0) = f \tag{5}$$

The scalar μ is our bifurcation indicator and determining a stationary bifurcation point consists in finding, for which Reynolds number λ, this scalar is null.

The previous system of equations is solved by using the Asymptotic Numerical Method [1,2]. The unknown $X = (U^\lambda, \lambda, \Delta U, \mu)$ is then sought as an integro-power series with respect to a perturbation parameter, 'a'.

4. Asymptotic Numerical Method

The Asymptotic Numerical Method consists in searching for the unknowns of the nonlinear problem (4) in the form of a truncated Taylor expansion from a known and regular solution $X_0 = (U_0^\lambda, \lambda_0, \Delta U_0, \mu_0)$:

$$X = \sum_{i=0}^{i=P} a^i X_i \tag{6}$$

where P is the truncated order of the asymptotic expansions. The perturbation parameter 'a' is defined as the projection of the velocity increment $(u - u_0)$ on the tangent velocity u_1:

$$a = \langle u - u_0, u_1 \rangle \tag{7}$$

where the operator $\langle \cdot, \cdot \rangle$ indicates the Euclidian scalar product. The expansions are introduced into Eqs. (4) and (7) and by equating like powers of 'a', we obtain a set of linear problems:

Order 1:

$$\begin{cases} L_t\left(U_1^\lambda\right) = \lambda_1 F \\ \langle u_1, u_1 \rangle = 1 \\ L_t(\Delta U_1) = \mu_1 f - \left\{ Q\left(U_1^\lambda, \Delta U_0\right) + Q\left(\Delta U_0, U_1^\lambda\right) \right\} \\ \langle \Delta u_p, \Delta u_0 \rangle = 0 \end{cases} \tag{8}$$

Order p (with $2 \leqslant p \leqslant P$):

$$\begin{cases} L_t\left(U_p^\lambda\right) = \lambda_p F - \sum_{r=1}^{p-1} Q\left(U_r^\lambda, U_{(p-r)}^\lambda\right) \\ \left\langle u_p^\lambda, u_1^\lambda \right\rangle = 0 \\ L_t(\Delta U_p) = \mu_p f - \sum_{r=1}^{p} \left\{ Q\left(U_r^\lambda, \Delta U_{(p-r)}\right) + Q\left(\Delta U_{(p-r)}, U_r^\lambda\right) \right\} \\ \langle \Delta u_p, \Delta u_0 \rangle = 0 \end{cases} \tag{9}$$

where $L_t(\cdot)$ is the tangent operator defined with $L_t(\cdot) = L(\cdot) + Q(\cdot, U_0) + Q(U_0, \cdot)$. It should be noted that the previous linear problems (8) and (9) all have the same tangent operator and differ from their right-hand sides (which depend on the previous computed vectors).

Thus the computation of the unknowns $X = (U^{\lambda}, \lambda, \Delta U, \mu)$ needs only one matrix triangulation and $2 * P$ backward and forward substitutions, where P is the order of truncature of the polynomial approximations. Firstly, the quantities for the steady Navier–Stokes equations are computed, which means $(U_p^{\lambda}, \lambda_p)$ and secondly the quantities to study the stability of the nonlinear solutions $(\Delta U_p, \mu_p)$. Indeed, as the right-hand side of the linear problem governing the stability of the system depends, at the order p, on the vector U_p, the latter has to be solved after the computation of the steady solution.

These asymptotic expansions are replaced by equivalent rational approximations, called Padé approximants [18–20]:

$$X_{Padé,P}(a) - X_0 = \sum_{k=1}^{P-1} \frac{R_{(P-1-k)}(a)}{Q_{(P-1)}(a)} a^k X_k \tag{10}$$

where R_k and Q_k are polynomials of degree k. As can be seen, the fractions in (10) all have the same denominator Q_k. Representation (10) has been initially tested and evaluated in [21,22] and is generally preferred to limit the number of roots of the Padé's denominator, which are called the "poles" of Padé approximants. The rational representation (10) has a range of validity that is greater than the polynomial approximation (6) (generally twice as great) which is why this representation is chosen. The range of validity of the rational representation is simply determined by the following expression [23]:

$$\delta = \frac{\|U_{Padé,P}(a_{max\,Padé}) - U_{Padé}, (P-1)(a_{max\,Padé})\|}{\|U_{Padé,P}(a_{max\,Padé}) - U_0\|} \tag{11}$$

The previous expression leads to an evaluation of the maximum value of the path parameter $a_{max\,Padé}$ by requiring that the difference between two rational solutions (10) at consecutive orders remains smaller at the end of the step than a chosen parameter, δ. Finally, by computing the maximum value of the path parameter $a_{max\,Padé}$ and by introducing it in relation (10), one can compute a new starting point (U_0, λ_0) for the asymptotic expansions (6). Thus, a supplementary analytic part of the nonlinear solution can be computed. One quite simply has to define a continuation method which leads to the determination of the whole solution of the steady Navier–Stokes equation (1).

Finally, ANM needs two user parameters, the first one being the truncature order P and the second one is the small parameter δ. The latter governs the accuracy of the computed nonlinear solutions. Usually, ANM needs no correction step at the end of the step. Nevertheless, for some values of the chosen parameter δ the accuracy of the solution obtained with ANM cannot be satisfactory. It means that the computed residual is greater than a given accuracy. In such a case, very efficient and cheaper correctors can be used at the end computation (see [24] or [25]) to improve the quality of the ANM solution.

Once all the unknowns are computed at each order, the polynomial expansions are replaced by Padé approximants. In this study, two Padé approximants are built, the first one for the couple of unknowns $(U_p^{\lambda}, \lambda_p)$ and the second one for the couple $(\Delta U_p, \mu_p)$. Therefore according to formula (11), two values of the validity range of the Padé approximants are computed. The first one based on the fundamental solution is denoted by $a^{\lambda}_{max\,Padé}$ and the second one which is computed from the perturbed vectors is denoted by $a^{\mu}_{max\,Padé}$. Finally, the smallest parameter $a^{\lambda}_{max\,Padé}$ or $a^{\mu}_{max\,Padé}$ is used to compute the new starting point $(U_0, \lambda_0, \Delta U_O, \mu_0)$. By choosing the smallest parameter, one ensures that both solutions (steady Navier–Stokes solutions and the perturbed quantities) evolve in the same way and are always in the range of validity of each asymptotic expansion.

In the previous works [3,5], the bifurcation mode and indicator were not sought in the form of an asymptotic expansion. The use of a perturbation method to compute the previous unknowns is a major feature compared to the previous works and should give more accurate values of the bifurcation point.

5. Detection of bifurcation points

When using ANM to compute steady nonlinear solutions, one can distinguish several possibilities to detect bifurcation points. The first and natural way is to use the bifurcation indicator. Indeed, as this indicator changes its sign when a bifurcation is encountered, an easy method is to numerically compute either the zero of the asymptotic expansions of the bifurcation indicator or the zero of the Padé approximants. Due to numerical instabilities, these zeros do not necessarily correspond to bifurcation points. Thus, once these zeros are computed, one must verify whether or not they also correspond to a steady solution by checking the accuracy, for example.

A second method to determine bifurcation points is to compute the indicator for several values of the path parameter (between 0 and $a^{\mu}_{max\,Padé}$) and if the indicator changes its sign then the instability point should be precisely determined by using, for example, a bisection method.

The third method comes from previous studies on ANM and more precisely on the analysis of the rational representation (10). It has been established in Ref. [26] that a bifurcation point corresponds to a root of the denominator, the so-called Padé poles, of the Padé approximants (10). Nevertheless, as Padé approximants have many poles (real or complex ones), one has to check if these poles really correspond to bifurcation points. Investigation, for example, must be limited to real poles.

In this study, the bifurcation points are determined by mixing the first and third methods, which means that during the whole computation (the steady solution and the indicator), the roots of the indicator and the poles of steady solutions are

computed. If both coincide then an instability point is found. Both previous conditions can be noted as satisfied by a bifurcation point and also by a turning point. In the latter case, one has to verify an additional condition which is:

$$\left.\frac{\mathrm{d}\lambda}{\mathrm{d}a}\right|_{a=a_c} = 0 \tag{12}$$

where a_c is the value of the path parameter a, which is a root of the indicator and also a pole of the steady solution.

The value of the path parameter, a_c, is introduced into the definition of the Padé approximants (10) and permits one to easily computes the fundamental solution and the bifurcation mode at the singular point, respectively denoted by U_c^λ and ΔU_c and defined by:

$$\begin{cases} U_c^\lambda(Padé) = U_0^\lambda + \sum\limits_{k=1}^{P-1} \frac{R^\lambda_{(P-1-k)}(a_c)}{Q^\lambda_{(P-1)}(a_c)} a_c^k U_k^\lambda \\ \Delta U_c(Padé) = \Delta U_0 + \sum\limits_{k=1}^{P-1} \frac{R^\mu_{(P-1-k)}(a_c)}{Q^\mu_{(P-1)}(a_c)} a_c^k \Delta U_k \end{cases} \tag{13}$$

where functions (R^λ, Q^λ) and (R^μ, Q^μ) are respectively the functions built from the fundamental or the perturbed solutions.

Finally, the numerical strategy used in this work to automatically compute the bifurcation points can be summarized by the following:

1. Compute the unknowns $X = (U^\lambda, \lambda, \Delta U, \mu)$ with the linear systems (8) and (9).
2. Build the Padé approximants with expressions (10), one for the stationary solution $(U^\lambda(Padé), \lambda(Padé))$ and one for the stability analysis $(\Delta U(Padé), \mu(Padé))$.
3. Determine the poles of the steady solution $U^\lambda(Padé)$, denoted by a_p.
4. Compute the roots of the bifurcation indicator $\mu(Padé))$, denoted by a_r.
5. If $a_p = a_r$, then the value a_r indicates a singular point.
   (a) If $\frac{\mathrm{d}\lambda}{\mathrm{d}a}|_{a=a_r} \neq 0$ then $a_c = a_r$ is a bifurcation point.
   (b) Else $a_c = a_r$ is a turning point, go to 1 for a new step of ANM.

In the following section, the proposed numerical method to compute the steady solutions emanating from the bifurcation points is presented.

6. Computation of the bifurcated branches

Once the steady bifurcation point is precisely determined by the zero of the indicator μ, we propose to compute the resulting bifurcated branches. In this study, two methods are used to compute these bifurcating branches. The first one, denoted by "Classical ANM" in the following, is to simply use the ANM and more precisely by varying the value of the two parameters (P, δ). Indeed these parameters play the roles of perturbation parameters and permit one to follow, according to their value, one bifurcated branch. By modifying their values, one can expect to follow all the post-bifurcation branches. The previous method is not very efficient and not automatic, but it is very simple. Moreover, reference curves can be gotten from it, which are then compared to the solutions obtained with the proposed algorithm.

The second method, denoted by "Proposed method" in the following, consists in determining exactly the bifurcated branches. It corresponds to the algorithm proposed in Ref. [4] for solid mechanics problems. Nevertheless, as the Navier–Stokes equations are non symmetric, some modifications have to be made for fluid mechanics problems. Hence, the bifurcation point, denoted by $(U_c^\lambda, \lambda_c, \Delta U_c)$ is supposed to be known. From this singular point, the nonlinear solution is sought in the form of an asymptotic expansion:

$$\begin{cases} U = U_c^\lambda + \sum\limits_{i=1}^{i=P} a^i U_i^\lambda \\ \lambda = \lambda_c + \sum\limits_{i=1}^{i=P} a^i \lambda_i \end{cases} \tag{14}$$

The previous expressions are introduced in Eqs. (2) and (7) and by equating like powers of 'a', we obtain a set of linear problems. For an order of truncature equal to 1, the corresponding linear system is written:

$$\begin{cases} L_t^c(U_1^\lambda) = \lambda_1 F \\ \langle u_1^c, u_1^c \rangle = 1 \end{cases} \tag{15}$$

where $L_t^c(\cdot)$ represents the operator tangent computed at the bifurcation point (U_c^λ, λ_c). As this operator is singular, the unknown U_1^λ is sought as a linear combination of a multiple of the bifurcation mode, $\eta_1 \Delta U_c$ where η_1 is an unknown scalar, and of a particular solution denoted by $\lambda_1 W$, as explained in Ref. [4,27]. Hence, the vector U_1^λ is then defined by:

$$U_1^\lambda = \lambda_1 W + \eta_1 \Delta U_c \tag{16}$$

Moreover, as a new unknown is introduced (*i.e.* W), the following orthogonality condition is added:

$$\langle W, \Delta U_c \rangle = 0 \tag{17}$$

Expression (16) is introduced in Eq. (15) which becomes:

$$L_t^c(W) = F \tag{18}$$

As the latter equation is also singular, we will see in the discrete part of this paper (see Section 7) how the vector W can be determined. The bifurcation mode satisfies the following relation:

$$L_t^c(\Delta U_c) = 0 \tag{19}$$

The two scalars, λ_1 and η_1, are determined by projecting the linear problem obtained at the order 2 on the left eigenvector, Φ, at the bifurcation point. The latter satisfies the following relation:

$${}^t\Phi L_t^c(Y) = 0 \quad \forall Y \in \mathbb{R}^3 \quad \text{and} \quad {}^t\Phi \Delta U_c = 1 \tag{20}$$

As for the vector W, the computation of the left eigenvector Φ requires particular attention (see Section 7). To compute the two scalars, the linear system to be solved at the order of truncature equal to 2 is written:

$$L_t^c\left(U_2^\lambda\right) = \lambda_2 F - Q\left(U_1^\lambda, U_1^\lambda\right) \tag{21}$$

By projecting the previous equation in the left eigenmode, ϕ, and by using the relations (18) and (20), one obtains:

$$\left\langle \phi, Q\left(U_1^\lambda, U_1^\lambda\right) \right\rangle = 0 \tag{22}$$

The definition of the vector U_1^λ (Eq. (16)) is introduced into the latter equation and the bifurcation equation is written:

$$\lambda_1^2 d + \lambda_1 \eta_1 c + \eta_1^2 b = 0 \tag{23}$$

with the following definition of the constants:

$$\begin{cases} b = \langle \phi, Q(\Delta U_c, \Delta U_c,) \rangle \\ c = \langle \phi, Q(W, \Delta U_c) + Q(\Delta U_c, W) \rangle \\ d = \langle \phi, Q(W, W) \rangle \end{cases} \tag{24}$$

Finally, the parameter λ_1 is simply determined by solving the quadratic equation (23):

$$\lambda_1^{1,2} = \eta_1 \frac{-c \pm \sqrt{c^2 - db}}{d} \tag{25}$$

By introducing the expression of scalar λ_1 into the second equation of (15), two couples of values $(\lambda_1, \eta_1)^{1,\,2}$ can be defined. Finally, the computation of the two previous couples permits ones to define the two tangents at the bifurcation point.

As, we want to compute all the nonlinear solution branches emanating from bifurcation point U_c^λ, all the other terms of the asymptotic expansions (14) must be determined. Hence, the linear problem satisfied by the unknowns at the order of truncature equal to p is written:

$$\begin{cases} L_t^c\left(U_p^\lambda\right) = \lambda_p F - \sum_{r=1}^{p-1} Q\left(U_r^\lambda, U_{(p-r)}^\lambda\right) \\ \left\langle u_p^\lambda, u_1^\lambda \right\rangle = 0 \end{cases} \tag{26}$$

As for the first order (Eq. (16)), the unknown, U_p^λ, is sought under the following form:

$$U_p^\lambda = \lambda_p W + \eta_p \Delta U_c + \widehat{U}_p \tag{27}$$

By introducing the relation (27) into linear problem (26) and by using relations (18) and (19), one obtains:

$$L_t^c\left(\widehat{U}_p^\lambda\right) = -\sum_{r=1}^{p-1} Q\left(U_r^\lambda, U_{(p-r)}^\lambda\right) \tag{28}$$

The computation of $\widehat{U}_p^\lambda$ is realized with a specific procedure as explained in Section 7. The two unknowns (λ_p, η_p) are determined by projecting problem (26) written at order $p+1$ on the left eigenmode Φ. The second required equation is obtained by using the path parameter definition (Eq. (7)). Finally, the two scalars (λ_p, η_p) verify the following linear system of equations:

$$\begin{bmatrix} \left\langle \Phi, \widetilde{Q}\left(U_1^\lambda, W\right) \right\rangle & \langle \Phi, \widetilde{Q}(\Delta U_c, W) \rangle \\ \left\langle W, U_1^\lambda \right\rangle & \left\langle \Delta U_c, U_1^\lambda \right\rangle \end{bmatrix} \begin{Bmatrix} \lambda_p \\ \eta_p \end{Bmatrix} = \begin{Bmatrix} -g \\ -\left\langle \widehat{U}_p^\lambda, U_1^\lambda \right\rangle \end{Bmatrix} \tag{29}$$

with the following definitions:

$$\begin{cases} \widetilde{Q}(a,b) = Q(a,b) + Q(b,a) \\ g = \left\langle \Phi, \widetilde{Q}\left(U_1^\lambda, \widehat{U}_p^\lambda\right)\right\rangle + \frac{1}{2}\sum_{J=2}^{p-1}\left\langle \Phi, \widetilde{Q}\left(U_J^\lambda, U_{(P+1-J)}^\lambda\right)\right\rangle \end{cases} \tag{30}$$

Finally, the previous equations make the computation of all the unknowns $(\lambda_p, \eta_p, U_p^\lambda)^{1,2}$ possible. These two values of the unknowns define two stationary bifurcated branches. By introducing these values into the asymptotic expansions (14) and by giving a positive or a negative value of the path parameter 'a', 4 bifurcated branches can be built from the bifurcation point (U_c^λ, λ_c). As for the stationary and linear stability analysis, Padé approximants are built from these asymptotic expansions and permit the range of validity of the polynomial expansions to be increased. In the following section, some precisions are given on how all these quantities are numerically computed.

7. Discretization step

Spatial discretization of the previous equations are performed by using the classical finite element method. The chosen finite element is a quadrilateral element, with 9 nodes for the velocity (bi-quadratic interpolation) and 3 for the pressure (linear interpolation) [28]. The continuity equation is solved by using a penalty method [28]. For the sake of simplicity, discrete and continuous quantities have the same names.

Concerning the stationary solution and the bifurcation indicator, the discrete problem to be solved at each order is written:

$$\begin{cases} K_t\left(U_0^\lambda\right)\cdot U_p^\lambda = \lambda_p F - FQ^\lambda\left(U_k^\lambda\right) \\ {}^t u_p^\lambda u_1^\lambda = 0 \\ K_t\left(U_0^\lambda\right)\cdot \Delta U_p = \mu_p f - FQ^\mu\left(U_p^\lambda, U_k^\lambda, \Delta U_k\right) \\ {}^t \Delta u_p \Delta u_0 = 0 \end{cases} \tag{31}$$

where $K_t(U_0^\lambda)$ is the tangent matrix. The right-hand side vectors (r.h.s.) $FQ^\lambda(U_k^\lambda)$ and $FQ^\mu(U_p^\lambda, U_k^\lambda, \Delta U_k)$ depend on the previous known solutions U_k^λ and ΔU_k (with $1 < k < p-1$) and also for the second r.h.s. on the fundamental solution at order p, U_p^λ. These r.h.s. correspond to the discretization of the second parts of the set of linear equation (9).

The previous linear systems lead to the computation of the fundamental solution and also to the quantities (μ and ΔU) required to study the stability of the flow. It should be noted that only a single matrix triangulation is needed to compute the two asymptotic expansions. The number of linear systems to be solved to determine all the terms of the asymptotic expansions (6) is equal to $2P$, P being the order of truncature. These computations are classical and are explained in details, for the stationary flow, in Ref. [2]. Finally all the discrete unknowns, $\left(U_p^\lambda, \Delta U_p, \mu_p\right)$, are computed. With these asymptotic expansions, the corresponding Padé approximants are determined. By studying the roots or the poles of these rational functions (as explained in Section 5) one can determine the singular points in the flow.

The numerical difficulty of the presented work comes from the computations of the quantities W, $\widehat{U}_p^\lambda$ and Φ at the bifurcation point. These vectors are solutions to a linear system whose matrix operator is singular. For example, for vector W, the discrete system to be solved corresponding to Eq. (18) is:

$$K_t^c\left(U_c^\lambda\right) W = F \tag{32}$$

where $K_t^c(U_c^\lambda)$ is the singular tangent matrix computed at bifurcation point U_c^λ (Eq. (14)). To compute vector W, the following augmented system (see [4,6]) is introduced:

$$\begin{bmatrix} K_t^c\left(U_c^\lambda\right) & \Delta U_c \\ {}^t\Delta U_c & 0 \end{bmatrix} \begin{Bmatrix} W \\ k \end{Bmatrix} = \begin{Bmatrix} F \\ 0 \end{Bmatrix} \tag{33}$$

The previous linear system is regular and the unknown W can be computed by doing the triangulation of the matrix. The computations of the vectors $\widehat{U}_p^\lambda$ at each order p is done with an augmented system which differs only with system (33) from the r.h.s. Thus only a single matrix triangulation is needed to compute vectors W and $\widehat{U}_p^\lambda$.

The calculus of the left eigenmode Φ requires the definition of a different augmented system than the one defined in (33). Indeed, according to relations (20), this augmented system is written:

$$\begin{bmatrix} {}^t K_t^c\left(U_c^\lambda\right) & \Delta U_c \\ {}^t\Delta U_c & 0 \end{bmatrix} \begin{Bmatrix} \Phi \\ k \end{Bmatrix} = \begin{Bmatrix} 0 \\ 1 \end{Bmatrix} \tag{34}$$

Finally the previous equations forward the computation of the stationary solutions and the bifurcation indicator (Eq. (31)) on the one hand, and the quantities needed to follow the bifurcating nonlinear solution branches (Eqs. (33) and (34)) on the other. Thus, two augmented matrix triangulations and P backward and forward substitutions are required to compute the

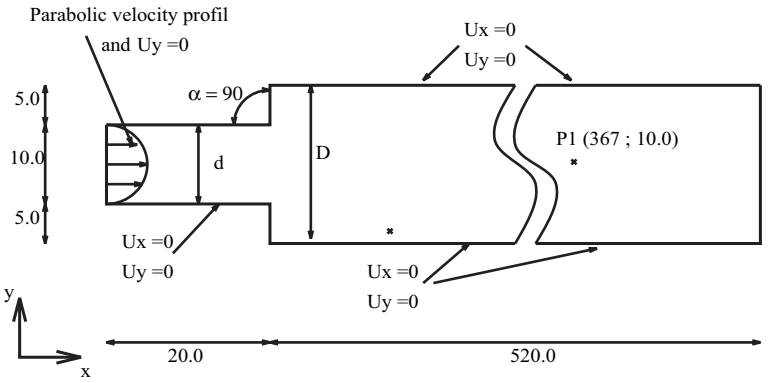

Fig. 1. Configuration and boundary conditions for the flow in a sudden expansion.

Table 1
Comparison of the critical Reynolds numbers from the literature for the flow in a sudden expansion (Fig. 1). Exp. and Num. stand for, respectively, experimental and numerical methods. For the latter the following acronyms (DNS), (EC) and (I), respectively mean direct numerical simulation, eigenvalue computation and indicator of bifurcation.

	Method		1st bif.	2nd bif.	3rd bif.
Cadou et al. [3]	Num. (I)		214–215	–	–
Allery et al. [5]	Num. (I)		213.6	–	–
Alleborn et al. [7]	Num. (EC)		218	542	–
Battaglia et al. [8]	Exp. & Num. (DNS)		217	–	–
Drikakis [10]	Num. (DNS)		216	–	–
Battaglia et al. [30]	Num.	–	215.4	–	–
Shapira et al. [31]	Num. (EC)		212.2–216	–	–
Wahba [32]	Num.	–	217.5	–	–
Cherdron et al. [33]	Exp.		$\geqslant$185	–	–
This study		FB1	215.63	–	–
		FB2	–	537.40	–
		FB3	–	–	946.47

four bifurcated branches. The CPU time needed for a triangulation of the augmented matrix is nearly the same as the one required for the computation of the fundamental branch. Indeed, the size of the augmented matrices is (ndof + 1) $\times$ (ndof + 1), whereas the size of the fundamental solution is ndof $\times$ ndof (ndof being the number of degrees of freedom of the numerical example). In the following section, classical numerical tests in fluid mechanics are studied to assess the efficiency and the applicability of the proposed numerical methods.

8. Numerical results

8.1. Numerical examples

In this section, three numerical tests exhibiting stationary bifurcation are evaluated with the proposed algorithms. The first example is the flow in a sudden expansion. The geometric configuration and the boundary conditions are given in Fig. 1. Here, we only consider the case with an expansion ratio $E = \frac{D}{d}$ equal to 2. Several authors have reported critical Reynolds numbers of the flow for which the stationary bifurcation appears. These reference Reynolds numbers are reported in Table 1. For this example, the Reynolds number is computed from the following relation: $Re_c = \frac{u_{\max} d}{\nu}$. $u_{\max}$ is the maximum of the parabolic profile of velocity in the entrance of the channel. d represents the height of the channel entrance and ν is the kinetic viscosity. The second example is the flow in a channel (see Fig. 2) and is the same as the one studied in references [9,29]. For this example, the aspect ratios, A, defined by $A = \frac{L}{3h}$, is introduced. Two values of this aspect ratio are studied ($A = \frac{7}{3}$ and $A = \frac{8}{3}$). The critical Reynolds numbers obtained in references [9,29] are summarized in Table 2 and are defined by $Re_c = \frac{u_{\max} h}{2\nu}$ where h is the height of the channel entrance. For all the numerical examples, the critical Reynolds numbers reported in Tables 1 and 2 have been recalculated to be consistent with our definitions.

For the three examples, the finite element used is a quadrilateral element, with 9 nodes for the velocity (bi-quadratic interpolation) and 3 for the pressure (linear interpolation) [28]. The corresponding number of degrees of freedom for each example is given in Table 3.

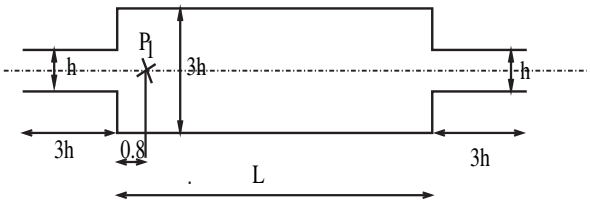

Fig. 2. Configuration and boundary conditions for the flow in a channel [9]. The aspect ratio A is defined by $A = \frac{L}{3h}$.

Table 2
Comparison of the critical Reynolds numbers from the literature for the flow in a channel (Fig. 2). Num. stands for and numerical methods with the following acronym (DNS) meaning direct numerical simulation.

		Method		1st bif.	2nd bif.
$A = \frac{7}{3}$	Mizushima [9]	Num. (DNS)		47.70	65.24
	Patel and Drikakis [29]	Num. (DNS)		45–47.4	65–70
	This study		FB1	48.74	–
			FB2	–	65.13
			BB11	–	65.11
			BB12	–	65.15
$A = \frac{8}{3}$	Mizushima [9]	Num. (DNS)		41.14	111
	This study		FB1	41.75	–
			FB2	–	105.96
			BB11	–	111.21[a]
			BB12	–	111.21[a]

[a] A turning point is found for this Reynolds number.

Table 3
Meshes used for the numerical examples.

Name	Description	Number of dof
Example 1	Flow in a sudden expansion	5542
Example 2	Flow in a channel [9], $A = \frac{8}{3}$	22,242
Example 3	Flow in a channel [9], $A = \frac{8}{3}$	24,682

8.2. Bifurcation points

The first numerical results we present concern the bifurcation indicator.For the first example (Flow in a sudden expansion, Fig. 1), where the first bifurcation is for a Reynolds number close to 215 (see Table 1), we begin the computations with a Reynolds number equal to zero. In Fig. 3, the evolution of the bifurcation indicator is plotted versus the Reynolds number. One can see in this figure that the indicator crosses the horizontal axis for a Reynolds number greater than 200 indicating then that a steady bifurcation occurs. To determine precisely the critical Reynolds number, the Proposed method, which is based on the poles of the steady solution and of the roots of the indicator is used. In Table 4, these critical Reynolds numbers are reported for several values of the ANM parameters (P, δ). P is the order of truncature of the polynomial expansions (6) and δ is the parameter governing the resulting accuracy of the ANM solutions.

In this table, the order of truncature changes from 10 to 30, whereas δ varies from 10^{-4} to 10^{-8}. From these computations, the critical Reynolds number seems to be close to $Re_c \approx 215$. Indeed, out of the 12 computations reported in Table 4 only 3 calculi give a critical Reynolds number not equal to 215. From these results, it seems to be preferable to use an accuracy parameter δ greater than 10^{-4} associated with an order of truncature greater than 15. In Ref. [4], the authors also obtain the same conclusions: choosing an order of truncature greater than 20 and a small value of parameter δ. The results reported in Table 4 show that the Proposed method is reliable because 9 computations give nearly the same critical Reynolds number.

In this table, we also indicate for each calculus the ANM step for which the critical Reynolds number is determined. Hence, one can estimate the CPU time required for the stability analysis with the Proposed method. The previous CPU time is determined by adding the CPU times required for the matrices triangulation (one per step) and for the computation of the solution of the $2 * P$ linear systems (Eq. (31)). The CPU time needed for a classical method to study the stability of the flow is also indicated in Table 4. More precisely, the eigenvalues of the tangent stiffness matrix are computed for two values of the Reynolds number with ARPACK [34]. By checking if an eigenvalue becomes null between these two values, the critical Reynolds number can then be estimated. For this example and for a Reynolds number equal to 213, the smallest real eigenvalue

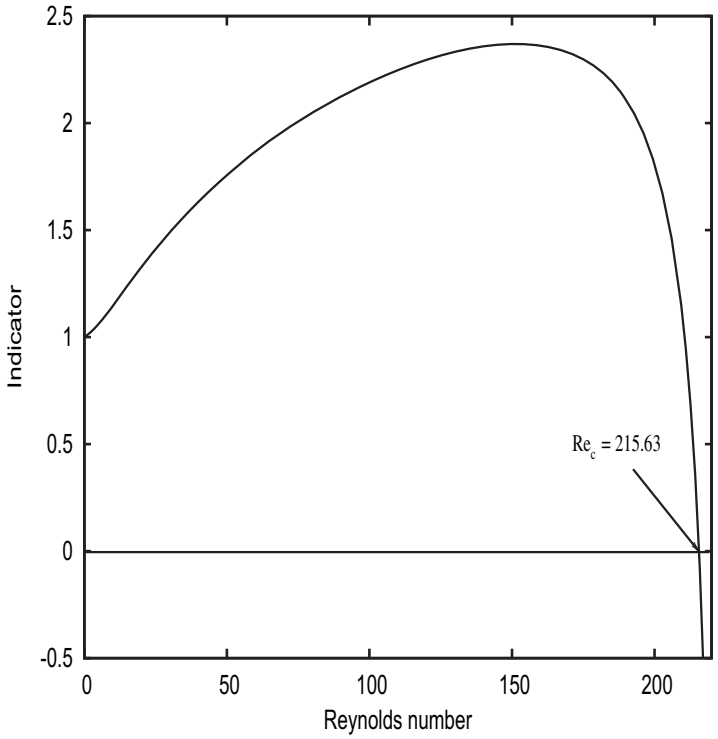

Fig. 3. Bifurcation indicator versus the Reynolds number. Flow in a sudden expansion.

Table 4
Critical Reynolds numbers for the flow in a sudden expansion (Fig. 1) versus ANM parameters (P, δ).

	P	δ	Re_c1	ANM step	CPU times (s)
Proposed Method	10	10^{-4}	215.63	6	4.0
	15	10^{-4}	215.63	5	5.2
	20	10^{-4}	219.91	9	13
	30	10^{-4}	218.46	8	18.8
	10	10^{-6}	216.47	11	7.4
	15	10^{-6}	215.63	7	7.3
	20	10^{-6}	215.66	5	7.2
	30	10^{-6}	215.63	4	9.4
	10	10^{-8}	215.31	18	12.2
	15	10^{-8}	215.64	9	9.4
	20	10^{-8}	215.89	6	8.6
	30	10^{-8}	215.63	5	11.7
ARPACK [34]	11	10^{-4}	213–217	–	260

is equal to -0.00012, whereas for $Re = 217$ the smallest eigenvalue is positive and equal to 7.7810^{-5}. Therefore, a steady bifurcation happens between these two Reynolds numbers. Thus, in Table 4, we indicate the CPU time (260 s) needed to compute these eigenvalues for these two Reynolds numbers. This time is relatively great which can be explained by the fact that the computation of more than 200 eigenvalues is necessary to determine the smallest real part values in the spectrum. In comparison, the CPU time required with the Proposed method is very small (from 4 s to nearly 20 s). Nevertheless, the solver ARPACK gives all the eigenvalues (the real and the complex ones) and makes it possible to see if another kind of bifurcation, for example Hopf bifurcation, happens. With the proposed algorithm, only steady bifurcation can be detected. For Hopf bifurcation, numerical methods also based on the ANM are available [3,13,14].

Finally, as suggested in Ref. [4] and shown in previous results, the ANM parameters are fixed and equal to ($P = 30$, $\delta = 10^{-8}$). Even if with these values, the computational times are not the lowest (see Table 4), the performed numerical tests show us that they lead to a very reliable algorithm in the detection of a bifurcation point. These parameters have been used to study the stability of the two other examples (Flow in a channel with $A = \frac{7}{3}$ and $A = \frac{8}{3}$). For these examples and for the considered meshes, the first steady bifurcation takes place for a Reynolds number equal to 48.74 and 41.75 respectively

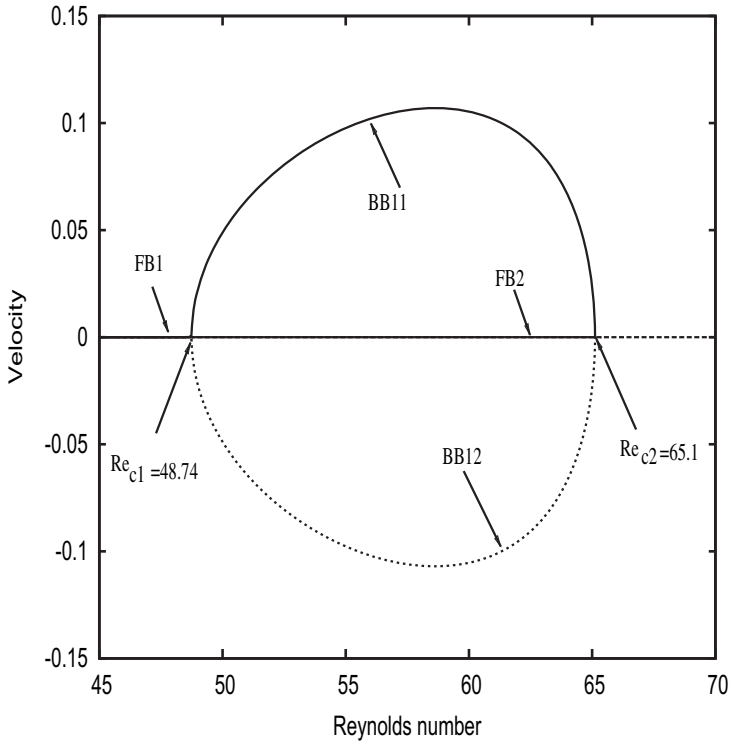

Fig. 4. Velocity u_y versus the Reynolds number. Bifurcated branches and critical Reynols number. The computations are done with the Classical ANM. Flow in a channel [9], case $A = 7/3$.

for $A = \frac{7}{3}$ and $A = \frac{8}{3}$ (see Table 2). These critical values are relatively close to the results of the literature. Once the critical Reynolds numbers are found, we propose to determine and follow the bifurcated branches.

8.3. Computation of the bifurcated branches

The flow in a channel with an expansion ratio $A = 7/3$ is considered. To compute the steady bifurcated branches after the bifurcation points, we propose two numerical methods. The first one is the Classical ANM. Actually, according to the values of the ANM parameters (P and δ), the numerical solution can switch to a bifucated branch or stay on the fundamental solution. In fact, these parameters play the role of numerical perturbation or numerical default and help to automatically follow bifurcated branches. The same numerical algorithm has been used in Refs. [3,5] to compute steady bifurcated solutions and is denoted by "Classical ANM" hereafter. The second method, denoted by "Proposed method", is the one presented in Section 6 and consists in exactly solving the nonlinear problem at the singular point. In Fig. 4, the bifurcated branches computed with the Classical ANM are plotted for the flow in a channel ($A = 7/3$). These plots correspond to the velocity Uy of the point P1 of Fig. 2. In Fig. 4, the following notation has been used. The fundamental solution is denoted by FBl where l indicates the l^{th} bifurcation. Whereas the bifurcation branches are called BBlm where m is equal to 1 for 'positive' velocity and equal to 2 for 'negative' velocity. The same notations are used for the other two examples. These nonlinear solutions are obtained in Fig. 4 with Classical ANM by varying the values of the parameters (P, δ). For example, to obtain the solutions FB1, FB2 and BB11, the order of truncature P is equal to 20 and the parameter δ is equal to 10^{-5}. The nonlinear branch BB12 is obtained with the following couple of values ($P = 15$, $\delta = 10^{-7}$).

These nonlinear branches can also be determined with the proposed method: computations of the 'exact' nonlinear solutions emanating from the bifurcation point with the method described in Section 6. Thus in Fig. 5, the solutions obtained with the two methods are plotted close to the first bifurcation point ($Re_c1 = 48.74$). The nonlinear branches computed with the Proposed method are denoted by 'branch 1' and 'branch 2' in this figure. Only bifurcated branches obtained with the Proposed method are plotted in this figure. The two other fundamental branches are not drawn. Moreover, branches 1 and 2 are determined with only one step of the perturbation method. One can also remark that in Fig. 5, branch 1 and BB11 are not as close to each other. In fact, as BB11 is obtained with ANM parameters which play the role of numerical perturbation, this solution is not as accurate near the bifurcation point. A similar behavior is observed in buckling problems when a default is introduced [16].

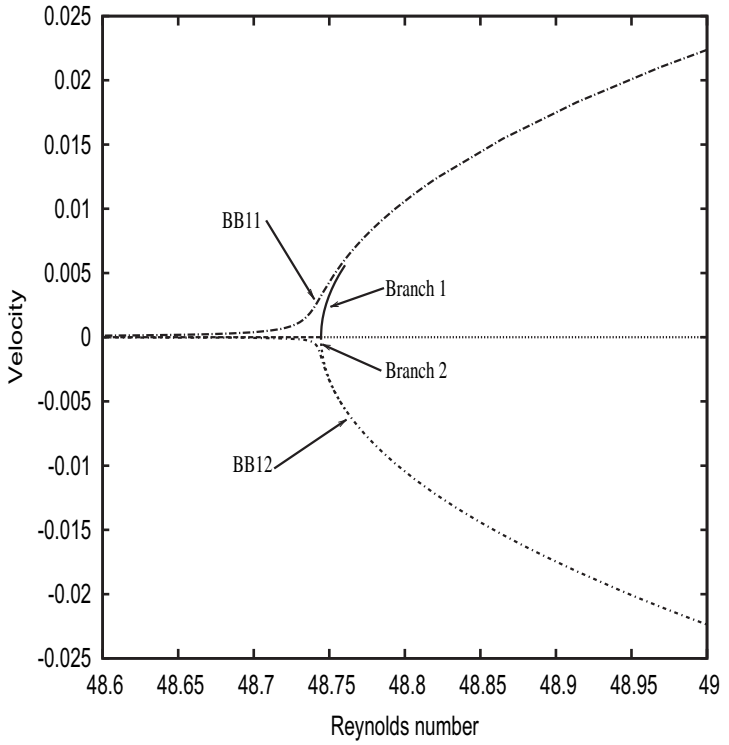

Fig. 5. Velocity u_y versus the Reynolds number. Bifurcated branches computed with the Classical ANM and the Proposed method at the first bifurcation point $Re_{c1} = 48.74$. Flow in a channel [9], case $A = 7/3$.

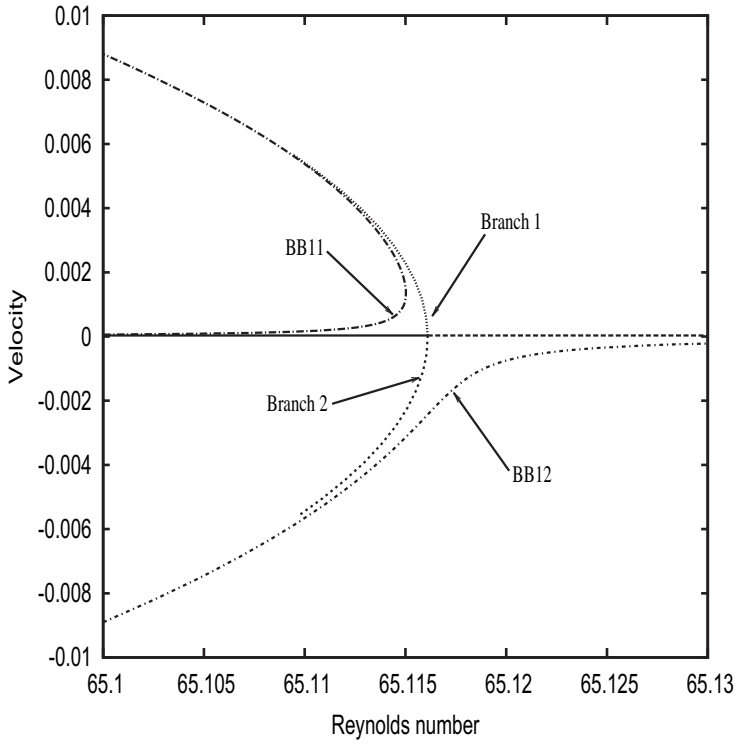

Fig. 6. Velocity u_y versus the Reynolds number. Bifurcated branches computed with the two methods at the second bifurcation point $Re_{c2} = 65.11$. Flow in a channel [9], case $A = 7/3$.

Table 5
Comparison of the performances of the two methods to compute the nonlinear branches of Fig. 4. Flow in a channel [9], case $A = 7/3$. N1, N2 and N3 are respectively the number of steps, the number of linear problems solved and the number of augmented matrix triangulated.

Method	Branch	P	δ	N1	N2	N3	CPU (s)
Classical ANM	FB1–FB2–BB11	20	10^{-5}	30	600	–	
	BB12	15	10^{-7}	20	300	–	
	Total			50	900	–	360
Proposed method	FB1	30	10^{-8}	4	2×120	2	
	FB2	30	10^{-8}	4	2×120	2	
	BB11	30	10^{-8}	5	2×150		
	BB12	30	10^{-8}	6	2×180		
	Total			19	1260	4	354

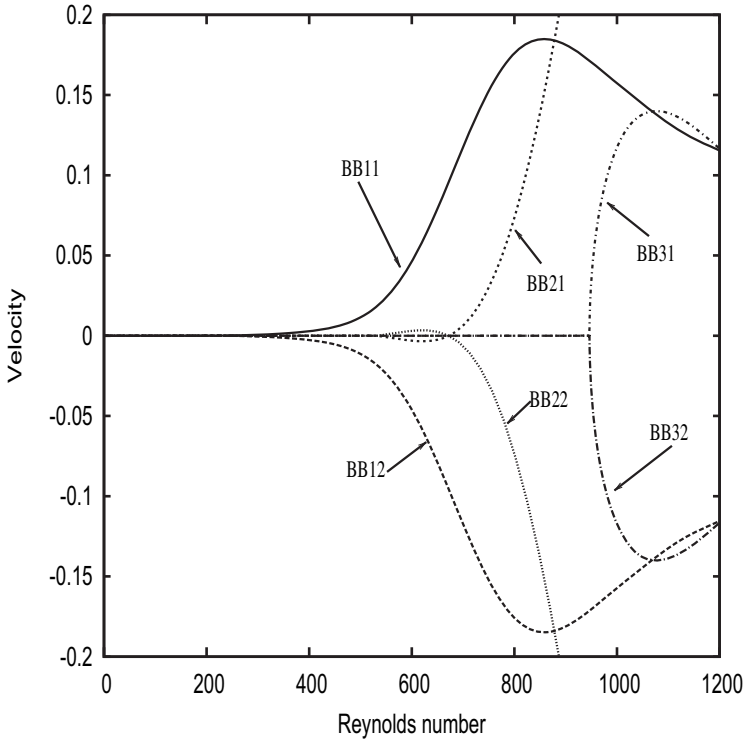

Fig. 7. Velocity Uy (Point P1 in Fig. 1) versus the Reynolds number. The different bifurcated branches are obtained with several couples of ANM paramaters, Classical ANM. Flow in a sudden expansion.

By taking the final point in the branches 1 and 2 (and also in the 3rd branch which is the 'positive' fundamental solution) as an initial point for a new computation with the Proposed method, one can compute another part of the solution and determine supplementary bifurcation points. These computations have been done for the three previous branches and a second bifurcation point has been found for a Reynolds number equal to 65.11 (see Table 2). The same critical Reynolds number is determined for the three computations and correspond well with the results found in the literature. In Fig. 6, the bifurcated branches obtained at this second bifurcation point are plotted and compared with the solutions obtained with the Classical ANM procedure. Finally, we compare, in Table 5, the performance of both methods to obtain the nonlinear solutions up to a Reynolds number equal to 65 for this example.

Both methods require approximatively the same CPU time (about 350s). Nevertheless, the number of steps is greater with Classical ANM than with the Proposed method, respectively 50 and 19. In fact, close to singular points, a step accumulation is observed when using the Classical ANM. In previous papers (see Refs. [2,16] for example), this propriety has been used to detect singular points, it is a 'visual' bifurcation indicator. The number of linear systems to be solved is greater with the Proposed method, 1260, while it is 900 for Classical ANM, because each step needs two problems to be solved, one for the stationary solution and one for the bifurcation indicator. In the end, the CPU time is approximatively the same with both methods. Nevertheless, Classical ANM requires some couples of parameters that help compute different nonlinear branches.

Table 6
Values of the ANM parameters to obtain the bifurcated branches of Fig. 7 with Classical ANM. Flow in a sudden expansion.

Name (Fig. 7)	ANM parameters	
	δ	P
BB11	$5 \cdot 10^{-6}$	10
BB12	$6 \cdot 10^{-3}$	18
BB21	$7 \cdot 10^{-6}$	10
BB22	$8 \cdot 10^{-4}$	20
BB31	$5 \cdot 10^{-5}$	10
BB32	$2 \cdot 10^{-5}$	14

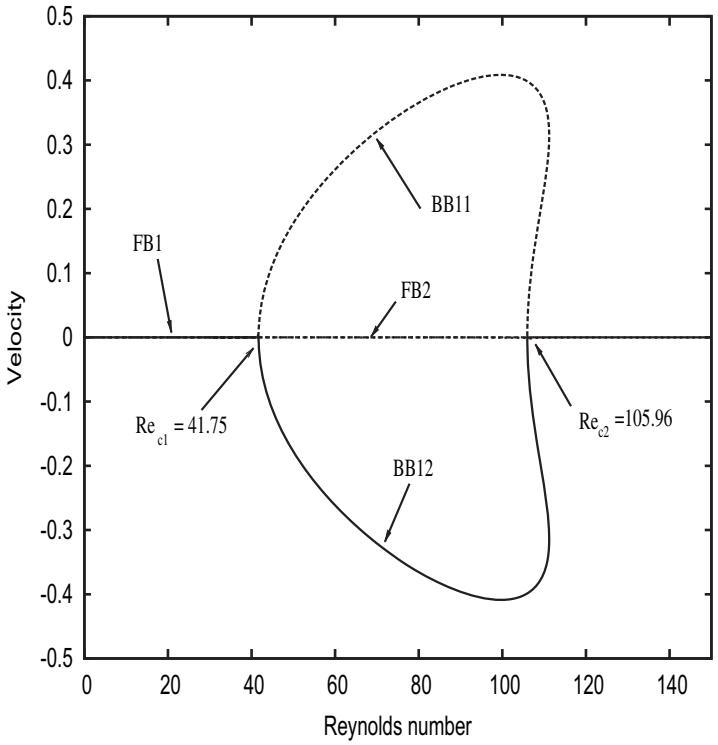

Fig. 8. Velocity u_y versus the Reynolds number. Bifurcated branches and critical Reynolds numbers. Flow in a channel [9], case $A = 8/3$.

Nevertheless, sometimes a great number of calculi are necessary to determine the efficient values of ANM parameters. For example, for the flow in a sudden expansion (see below) more than 700 calculi have been necessary to compute all the bifurcated branches of Fig. 7. Thus in Table 5, we present the "optimum" computational time for the Classical ANM.

One can also note in Table 5 that, for the Proposed method, four extended linear systems have been solved: two for each bifurcation point. The first one to compute vectors W and $\widehat{U}_p^{\dagger}$ (respectively Eq. (18) and (28)) and the second one to compute the left eigenvector, Φ (Eq. (20)).

We will now consider flow in a sudden expansion. In Fig. 7 we have plotted the nonlinear curves up to a Reynolds number equal to 1200. These curves are obtained with Classical ANM, but the same solutions are also obtained with the Proposed method. In Table 6, the values of the ANM parameters (P, δ) used to obtained all the branches of Fig. 7 are given. In this case, more than 700 calculi have been necessary to compute all these nonlinear branches. Indeed 700 couples of values of (P, δ) in the following ranges $10 < P < 40$ and $10^{-1} < \delta < 10^{-8}$ have been automatically tested. These numerous calculations lead to a huge amount of computational time compared to that of the Proposed method. Indeed with the latter, only 10 calculi are necessary to get all the nonlinear branches of Fig. 7 with the same couple of ANM parameters ($P = 30, \delta = 10^{-8}$). Moreover, with the Proposed method, three bifurcation points can be accurately determined (see Table 1). The first one, $Re_{c1} \approx 215$ is relatively well-known in the literature (see Table 1). The second bifurcation point $Re_{c2} \approx 537$ has only been reported to our knowledge in Ref. [7]. The third one, $Re_{c3} \approx 943$ has never been reported in the literature, perhaps because the flow becomes time periodic (via a Hopf bifurcation) for a Reynolds number close to 600 [35]. Moreover, as in Ref. [7], the three pre-

vious bifurcation points are determined on the fundamental branch. No bifurcation point has been detected on the bifurcated branches.

We will now consider the third example, the flow in a channel with an expansion ratio A equal to 8/3. The corresponding nonlinear response curves versus the Reynolds number are plotted in Fig. 8. These curves are obtained with the Proposed method. In Table 2, we give the critical Reynolds numbers computed with the bifurcation indicator. For this example, two bifurcation points are found, $Re_{c1} \approx 41$ and $Re_{c2} \approx 106$. The second bifurcation point has been detected on the fundamental branch FB2 (emanating from the first bifurcation point). On the two bifurcation branches, BB11 and BB12 (see Fig. 8), a turning point (satisfying relation (12)) is determined for each branch for a Reynolds number equal to 111. In Ref. [7], the authors have found that a second stationary bifurcation occurs for a critical Reynolds number close to 111. In fact, they could not accurately evaluate this second bifurcation point because they could not compute the unstable fundamental branch FB2 with their numerical method. With the proposed methods presented, stable and unstable branches can be computed. Nevertheless, one cannot assert if these branches are stable or unstable.

9. Conclusion

In this paper, several numerical methods to study the stability of fluid problems have been proposed. Firstly, a bifurcation indicator is introduced to determine the bifurcation points. The presented indicator has the property to be null in the bifurcation points. Compared to previous studies in fluid mechanics [3,5], the proposed method is quite different. Indeed, the bifurcation indicator is sought, as the stationary solution, in the form of an integro power series. The computation of this indicator is realized in parallel with the computation of the stationary solution. These asymptotic expansions are then replaced by equivalent rational fractions. Determining a bifurcation point consists in finding the roots of these rational approximations coupled with the 'poles' of the stationary solution. Finally, an automatic method to determine the critical Reynolds numbers of the flow is defined. As the stability is studied during the computation of the stationary nonlinear solutions, the additional computational time is low. Indeed no additional matrix triangulations are necessary, only supplementary linear systems have to be solved. The corresponding linear systems is twice what is needed to compute the fundamental solution with ANM. As in Ref. [4], the optimium ANM parameters seem to be a great order of truncature (P greater than 20) and a small accuracy parameter (δ lower than 10^{-6}). With these values, the Proposed method is very efficient and the numerical results correspond well with the results of the literature.

Secondly, as the bifurcation points are determined, a method to compute all the nonlinear bifurcated branches is proposed. ANM is also used but by taking some precautions in its application. Indeed, as the tangent matrix is singular in the bifurcation point, one has to define the extended system to compute the nonlinear branches. Moreover, the method requires the computation of the left eigenvector at the bifurcation point. Nevertheless, the Proposed method permits one to determine very accurately the nonlinear bifurcated solutions. Compared to Classical ANM, this method is very reliable and leads, with few calculi, to the determination of all the bifurcated nonlinear branches. Hence, one can study the stability on these nonlinear solutions and determine additional bifurcation points.

The proposed methods are only applied in this work to 2D-flows. Nevertheless, the application to the 3D case is not a difficult task. The only difficulty being the number of unknowns which is considerably increased when 3D flows are studied. The solution is, for example, to use specific linear solvers as in Ref. [12] or in Ref. [36]. In the latter, a linear solver which is well adapted to ANM is introduced and makes it possible to reduce the computational times.

The presented methods should help to easily study the influence of some geometric parameters on the stability of the flow as is done in Refs. [7,8,10,30]. This will be one of our future works. Hence, with the proposed algorithm, the influence of the geometric aspect ratios on the critical Reynolds numbers can be easily studied. For example, for the flow in a sudden expansion, the influence of the expansion ratio and the expansion asymmetry (see [7,37]) on the critical Reynolds numbers can be studied without difficulties. In this example, a small modification of the expansion asymmetric can have a great influence on the critical Reynolds numbers. For some values of this geometric parameter, the bifurcation vanishes and a limit point occurs. With the proposed algorithm, a geometric study can be easily done. One can also couple the present study with the algorithms presented in [13,14] to detect Hopf bifurcations on the stationary bifurcation branches and then determine all the instabilities in the flow with low computational time.

References

[1] B. Cochelin, A path-following technique via an asymptotic-numerical method, Comput. Struct. 53 (5) (1994) 1181–1192.
[2] J.M. Cadou, B. Cochelin, N. Damil, M. Potier-Ferry, Asymptotic Numerical method for stationary Navier–Stokes equations and with Petrov–Galerkin formulation, Int. J. Numer. Methods Eng. 50 (2001) 825–845.
[3] J.M. Cadou, M. Potier-Ferry, B. Cochelin, A numerical method for the computation of bifurcation points in fluid mechanics, Eur. J. Mech. B/Fluids 25 (2006) 234–254.
[4] E.H. Boutyour, H. Zahrouni, M. Potier-Ferry, M. Boudi, Bifurcation points and bifurcated branches by an asymptotic numerical method and Padé approximants, Int. J. Numer. Methods Eng. 60 (2004) 1987–2012.
[5] C. Allery, J.M. Cadou, A. Hamdouni, D. Razafindralandy, Application of the asymptotic numerical method to the Coanda effect study, Rev. Eur. Elém. Finis 13 (2004) 57–77.
[6] P. Vannucci, B. Cochelin, N. Damil, M. Potier-Ferry, An asymptotic-numerical method to compute bifurcating branches, Int. J. Numer. Methods Eng. 41 (1998) 1365–1389.

[7] N. Alleborn, K. Nandakumar, H. Raszillier, F. Durst, Further contributions on the two-dimensional flow in a sudden expansion, J. Fluid Mech. 330 (1997) 169–188.
[8] F. Battaglia, G. Papadopoulos, Bifurcation characteristics of flows in rectangular sudden expansion channels, J. Fluids Eng. 128 (2006) 671–679.
[9] J. Mizushima, H. Okamoto, H. Yamaguchi, Stability of flow in a channel with a suddenly expanded part, Phys. Fluids 8 (11) (1996) 2933–2942.
[10] D. Drikakis, Bifurcation phenomena in incompressible sudden expansion flows, Phys. Fluids 9 (1) (1997) 76–87.
[11] C.Y. Huang, F.N. Hwang, Parallel pseudo-transient Newton–Krylov–Schwarz continuation algorithms for bifurcation analysis of incompressible sudden expansion flows, Appl. Numer. Math. 60 (7) (2010) 738–751.
[12] M. Medale, B. Cochelin, A parallel computer implementation of the asymptotic numerical method to study thermal convection instabilities, J. Comput. Phys. 228 (22) (2009) 8249–8262.
[13] A. Brezillon, G. Girault, J.M. Cadou, A numerical algorithm coupling a bifurcating indicator and a direct method for the computation of Hopf bifurcation points in fluid mechanics, Comput. Fluids 39 (2010) 1226–1240.
[14] G. Girault, Y. Guevel, J.M. Cadou, An algorithm for the computation of multiple Hopf bifurcation points based on Padé approximants, Int. J. Numer. Methods Fluids, submitted for publication.
[15] E.H. Boutyour, Méthode Asymptotique Numérique pour le calcul de bifurcations: application aux structures élastiques, Ph.D. Thesis, Université de Metz, 1994 (in French).
[16] S. Baguet, B. Cochelin, On the behaviour of the ANM continuation in the presence of bifurcations, Commun. Numer. Methods Eng. 19 (2003) 459–471.
[17] A. Tri, B. Cochelin, M. Potier-Ferry, Résolution des équations de Navier–Stokes et détection des bifurcations stationnaires par une méthode asymtptotique-numérique, Rev. Eur. Elém. Finis 5 (1996) 415–442.
[18] G.A. Baker, P. Graves-Morris, Padé approximants, Encyclopedia of Mathematics and Its Applications, second ed., Cambridge University Press, Cambridge, 1996.
[19] A. Najah, B. Cochelin, N. Damil, M. Potier-Ferry, A critical review of asymptotic numerical methods, Arch. Comput. Methods Eng. 5 (1998) 3–22.
[20] N. Damil, J.M. Cadou, M. Potier-Ferry, Mathematical and numerical connections between polynomial extrapolations and Padé approximants, Commun. Numer. Methods Eng. 20 (9) (2004) 699–707.
[21] B. Braikat, N. Damil, M. Potier-Ferry, Méthodes asymptotiques numériques pour la plasticité, Rev. Eur. Elém. Finis 6 (1997) 337–357.
[22] A. Najah, B. Cochelin, N. Damil, M. Potier-Ferry, A critical review of asymptotic numerical method, Arch. Comput. Methods Eng. 5 (1) (1998) 3–22.
[23] A. Elhage-Hussein, M. Potier-Ferry, N. Damil, A numerical continuation method based on Padé approximants, Int. J. Solids Struct. 37 (2000) 6981–7001.
[24] H. Lahmam, J.M. Cadou, H. Zahrouni, N. Damil, M. Potier-Ferry, High order predictor–corrector algorithms, Int. J. Numer. Methods Eng. 55 (2002) 685–704.
[25] J.-M. Cadou, N. Damil, M. Potier-Ferry, B. Braikat, Projection techniques to improve high-order iterative corrector, Finite Elem. Anal. Des. 41 (2004) 285–309.
[26] B. Cochelin, N. Damil, M. Potier-Ferry, Asymptotic Numerical Method and Padé approximants for nonlinear elastic structures, Int. J. Numer. Method Eng. 37 (1994) 1187–1213.
[27] R. Seydel, From equilibrium to chaos, Practical Bifurcation and stability analysis, Springer-Verlag, New York, 1994.
[28] O.C. Zienkiewicz, R.L. Taylor, The Finite Element Method, fourth ed., vol. 2, McGraw-Hill Book Company, 1991.
[29] S. Patel, D. Drikakis, Prediction of flow instabilities and transition using high-resolution methods, in: Proceedings of the European Congress on Computational Methods in Applied Sciences and Engineering, ECCOMAS 2004.
[30] F. Battaglia, S.J. Tavener, A.K. Kulkarni, C.L. Merkle, Bifurcation of low Reynolds number flows in symmetric channels, AIAA J. 35 (1997) 99–105.
[31] M. Shapira, D. Degani, D. Weihs, Stability and existence of multiple solutions for viscous flow in suddenly enlarged channels, Comput. Fluids 18 (1990) 239–258.
[32] E.M. Wahba, Iterative solvers and inflow boundary conditions for plane sudden expansion flows, Appl. Math. Model. 31 (2007) 2553–2563.
[33] W. Cherdron, F. durst, J.H. Whitelaw, Asymmetric flows and instabilities in symmetric ducts with sudden expansion, J. Fluid Mech. 84 (1978) 13–31.
[34] R. Lehoucq, D.C. Sorensen, C. Yang, Arpack User's Guide: Solution of Large-Scale Eigenvalue Problems with Implicitly Restarted Arnoldi Methods, SIAM, Philadelphia, 1998.
[35] F. Durst, J.C.F. Pereira, C. Tropea, The plane symmetric sudden-expansion flow at low Reynolds number, J. Fluid Mech. 248 (1993) 567–581.
[36] J.M. Cadou, M. Potier-Ferry, A solver combining reduced basis and convergence acceleration with applications to non-linear elasticity, Int. J. Numer. Methods Biomed. Eng. 26 (2010) 1604–1617.
[37] R.M. Fearn, T. Mullin, K.A. Cliffe, Nonlinear flow phenomena in a symmetric sudden expansion, J. Fluid Mech. 211 (1990) 595–608.